THERMODYNAMIC TREATMENT FOR RELATIVISTIC HEAVY ION COLLISIONS

A. Alhaidary

Physics department faculty of science, Taiz University - yemen

Abstract

A phenomenological model is presented based on the formation of a nonequilibrium nuclear thermo-dynamic system during the collision of intermediate and high energy heavy ions. The formulation and the dynamic picture are determined by solving the Vlasov equation. The solution is dressed in the form of a power series, the first term of which being the equilibrium distribution in phase space. The rest, are time dependent perturbation terms due to the multiple strong interactions inside the system. The temperature gradient and the derivatives of the phase function are calculated. The time dependence of the angular emission of the produced particles is studied. It is found that particles emitted in the forward direction are produced in the early stage of the reaction, far from the equilibrium. Backward production comes in a later stage when the system constituents undergo multiple cascade collisions.

keywords: Non-equilibrium thermodynamic, heavy ion, high energy interactions.

1 Introduction

Heavy-Ion collisions at high energies produce large showers of different kinds of particles. Nucleons, pions and light nuclei are observed over a wide range of energy and angle. These various products seem to be associated with three relatively distinct sources (see Fig.2). These are the projectile spectator, the target spectator and an overlap region.In the more peripheral collisions substantial fragments of both the target and projectile may remain. These "spectators" may be highly excited, leading to particle emission (more or less isotropic in the rest frame of the fragment) and to a distribution of final products (evaporation residues). In addition, some sort of intermediate composite may be formed from those parts of nuclei that overlapped during the collision. Particles from this region should be distributed in velocity between the target and projectile if each particle experiences at least two or three collisions on the average, they also be spread fairly widely in angle. This part of the collision complex becomes more important with describing impact parameter. For central collisions where the entire projectile overlaps the target, no projectile "spectator" remains and most of the yield of the reaction is expected at intermediate energies and widely spread in angle [1]. The relative yields of the different products observed in this intermediate region and their energy and angular distributions can be estimated from simple geometric, kinematics and statistical considerations. Many theoretical models such as the fireball model [2] have been introduced to study the particle production in heavy ion collisions at medium energy, where the concept of global equilibrium may be accepted. The fireball model was developed to fit the

experimental data at higher energies. A local equilibrium was assumed in the so called fire-streak model [1, 3] that treats the variation, across the overlap region of the target and projectile, in the amount of energy and momentum that it deposited. The expression for calculating any observable takes the form of a sum over a series of terms, each one of which concerns a local equilibrium and consists of a geometric, kinematics and statistical factors. As the energy increases more, it is expected that collision time becomes small enough so that particle emitted in the early stage of the reaction possesses non-equilibrium characteristics. The density function in phase space should be treated on the time scale to follow up the time grow of the reaction. Many trials have been done in this concern. The equation of motion can be reformulated to give it the appearance of classical equation for the phase distribution function. In this approximation, a local one body potential can be defined and the phase distribution function may contain the same information as the one body density matrix. This is the Hartree-Fock approximation [4].

Many physical body physics enter only through the relation of the potential and the density. One more approximation reduces the equation to completely a classical form is to make a power series expansion of the one body potential and get the so called Vlasov equation [5, 6, 7]. A situation that can be analyzed with the Vlasov equation is the short time behaviour of the system subjected to an impulsive force. If the potential is sufficiently weak, the solution of the excited system may be treated by the quantum mechanical sum rules introduced first by Fallieros [8] and Noble [9]. While it is not possible to integrate the Vlasov equation in general, some insight may be given by expanding the solution for small intervals of time. The starting point is the equilibrium solution, which is perturbed by the impulsive potential. Another treatment of the Vlasov equation depends on the theory of small oscillations in finite system [10]. A closed expression has the appearance of Rayleigh's variation principle with a certain explicit form for the potential energy function. The solution is represented in the form of a sum of an equilibrium function plus a time dependent which is to be assumed small compared with the first. The motion is assumed to have a sinusoidal time dependence with frequency. The variational principle was applied to estimate the frequencies of nuclear vibrations of various multi-polarity. In this work a method is developed to solve the Vlasov equation with reasonable approximations in a frame of a time dependent thermodynamic model, which enables the calculations of light and heavy particle spectra on the different reaction stages. The details of the model are presented in the following sections.

2 The Formulation of the Model

Let us consider the collision between a target nucleus **T** and a projectile one **P** at a given impact parameter b. It is plausible to work with a parameter that defines the fraction of the projectile nucleons in the formed nuclear system as:

$$\eta(b) = \frac{\rho_{\mathrm{P}}(b)}{\rho_{\mathrm{P}}(b) + \rho_{\mathrm{T}}(b)} \tag{1}$$

where $\rho_P(b)$ and $\rho_T(b)$ are the projectile and target densities, respectively, at a given impact parameter b in the formed nuclear matter. $\eta(b)$ has continuous values extending from zero to 1. It is zero in the target region and goes to 1 as we approach the projectile region, as shown in Fig.(1).

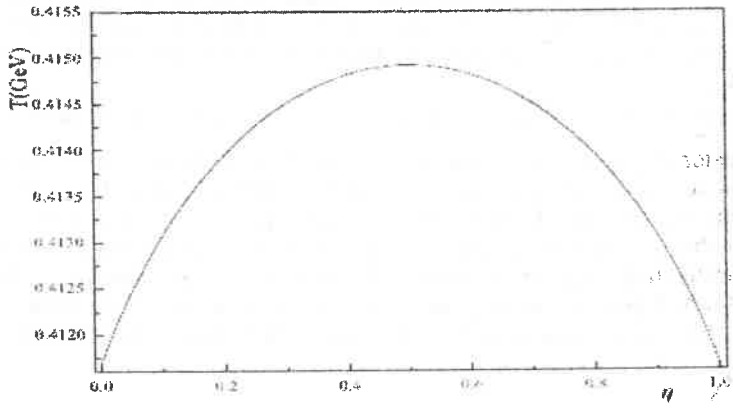

Figure.(1). The variation of the temperature as a function of the projectile density η for Mg-Em interaction at 3.6 GeV incident kinetic energies.

Considering a frame of reference coincides with the center of the target nucleus in the Laboratory system, the relative projectile density $\eta(r,b)$, at a distance r inside the fireball matter and an impact parameter, b, is given by

$$\eta(r,b)=\frac{\rho_P(r-b)}{\rho_P(r-b)+\rho_T(r-b)} \qquad (2)$$

The nuclear density, $\rho_i(r)$, of nuclei of mass number $A < 20$ can be calculated using the Gaussian distribution *i.e.*,

$$\rho_i(r)=A_i(\pi R_i^2)^{-3/2}\,Exp(-r^2/R_i^2) \quad i = \text{P, T} \qquad (3)$$

while for nuclei of $A \geq 20$, $\rho_i(r)$, can be calculated using the Fermi or Woods-Saxon distribution;

$$\rho_i(r)=\rho_\circ[1+Exp(\frac{r-c}{d})]^{-1} \qquad (4)$$

$$c_i=1.19A_i^{1/3}-1.61A_i^{-1/3} \quad \text{fm} \qquad i=\text{P,T}$$

where the surface thickness $d=0.54$ fm, and $\rho_\circ=0.159\ \text{GeV/fm}^3$.

The parameter η plays an important role in understanding the physics inside each part of the interacting medium as it controls the quantity of energy transferred and the activity of nuclear collisions.

In relativistic heavy ion collisions (RHIC), collision geometry determines features of observables. When the impact parameter, b, is about a sum of radii of the nuclei, both nuclei are touching on the surface at most closest point, and only the nucleons in this surface will be involved in the collisions. Such collision is called peripheral collision. On the contrary, when the impact parameter is zero, most of the nucleons will be involved in the collisions. Such an event is called central collision.

In a naïve geometrical picture of non-central collision, it is called participant – spectator model. There are three regions for colliding nuclei which are called the target spectator region, the hot spot (fireball) region, and the projectile spectator region. Schematic picture before, during, and after collision is shown in Fig.(2) (top and bottom drawings respectively). In the figure, impact parameter, b, is also shown. Nucleons in the overlapping region are called participants. The other remaining parts, which pass away from the fireball in the early stage of the collision, are called spectators.

2.1 The projectile spectator region

It is characterized by a small momentum transferred that is enough to dissociate the projectile into few fragments moving in the forward direction or scattered by relatively small angles. Simple elastic scattering [11] assuming optical potential [12, 13], diffraction [14] and Coulomb dissociation [15] models are sufficient to describe the fragmentation process and the angular spread of the emitted fragments in this region.

2.2 The target spectator region

The nucleons in this region are initially at rest. As the collision starts up, nucleons from the projectile defuse slowly through the target transferring a little bit fraction of the projectile energy. The diffusion rate depends mainly on the impact parameter. The system then behaves as perfect gas that suffers multiple of successive elastic scattering. Consequently the entropy of the system increases until it reaches equilibrium state, with equilibrium temperature of the order of 30 MeV. At this moment the system evaporates [16] producing heavily ionizing fragments which appear as black particles in nuclear emulsions with isotropic distribution in the space. In most cases it was sufficient to describe the energy distribution of the evaporated particles with a unique Maxwell distribution of classical distinguished particles.

2.3 The hot spot region

It is the overlapping region between the projectile and the target that characterizes with relative projectile density, $\eta \approx 0.5$. Also it is the hottest region in the space.

Large amount of heat is dissipated there. This naive geometrical picture is necessary to understand the observables because of the following two reasons:

1. Elementary process of nucleus - nucleus collisions is nucleon - nucleon collisions, because the de Broglie wavelength of incident nuclei is much shorter than the size of nuclei.

2. Each constituent nucleon collides dominantly with nucleons located in tubular region with about.

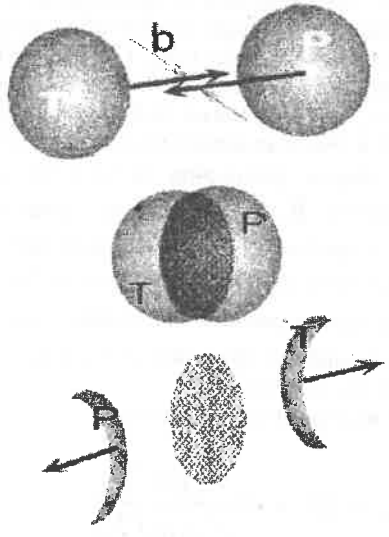

Figure 2: Schematic picture of relativistic heavy ion collision before (top), during (middle), and after (bottom) the collision. Note that the projectile (**P**) and the target (**T**) are Lorentz contracted in their center of mass frame. Hatched regions indicate hot and/or dense fireball. Impact parameter, b , is also shown.

nucleon radius and with length in the incident momentum direction. Because collision time is much shorter than the traversing time for a nucleon to reach the next (in perpendicular to incident momentum) nucleon. If we treat the system thermodynamically [17], it is expected that the collision goes through sequential stages. The first is a compression of the nuclear matter due to the high energy interaction, forming a fireball with diffuseness surface on the contrary of the fireball model assumptions which support the concept of the participant and spectator nucleons with pure cylindrical cut in the nuclear matter. Multiple nuclear collisions run inside the fireball which increase the energy density and allow the formation of quark gluon plasma state [18, 19, 20, 21]. This leads to the creation of new particles and expansion of the system which gradually approaches the equilibrium state. The last stage is the fireball decay. Particle emission from the fireball is allowed at different points on the time scale of the reaction. Light created particles are expected to be emitted on the early stage at narrow forward cone angle, i.e. due to the first

few collisions. The higher order collisions draw the system towards the equilibrium state producing particles in isotropic distribution in phase space. We treat the nuclear matter as a nonequilibrium system. Each point in the space is considered as a local equilibrium subsystem behaving as a canonical ensemble that is characterized by a specific temperature and a specific projectile fraction parameter η., Fermi-Dirac for fermions and Bose-Einstein for bosons [4].

It is then convenient to consider the state of equilibrium as a time reference of the reaction. Drawing back, we may follow the historical grow of particle emissions on the time scale. Hadronic matter inside the fireball is partially formed by the fast projectile nucleons and the slow target ones. The relative projectile density in this mixture is a very important parameter. It determines the fireball parameters, the center of mass velocity, the temperature and the temperature gradient inside the fireball matter. We use a Gaussian density distribution for nuclei of mass number A < 20, and a Woods-Saxon distribution for $A \geq 20$. Using appropriate units: $\hbar = c = k = 1$, where $\hbar, c, k$ are Planck's constant, speed of light and Boltzmann's constant, respectively [22]. On the other hand, since the center of mass itself is moving with velocity β_{cm} with respect to the laboratory system, related to its η value, then the emitted particles are produced with anisotropic decay. The degree of anisotropy depends on the center of mass velocity or the energy of the emitted particles. Then the center of mass
energy dissipated in a local position is given by:

$$\zeta_{cm} = 3T + m\frac{K_1(m/T)}{K_2(m/T)} \qquad (5)$$

Where T is the temperature in the unit of MeV and m is the nucleon rest mass. $K1$ and $K2$ are McDonald's functions of the first and second orders, respectively [23]. The conservation of energy at a given location requires that:

$$[m^2 + 2\eta(1-\eta)mt_i]^{1/2} = 3T + m\frac{K_1(m/T)}{K_2(m/T)} \qquad (6)$$

t_i is the incident kinetic energy per nucleon in the laboratory system. Eq.(6), is valid for each type of particles forming the fireball. Its solution results the value of the local temperature at the specific η value Fig.(1). It is assumed that at each local equilibrium point the occupation probability for the state with momentum P is given by Fermi-Dirac distribution appropriate for the temperature T. The number of particles in a volume V with momentum P within the interval dP is ;

$$dN = \frac{gV4\pi P^2 dP}{(2\pi)^3}\left\{\frac{1}{1+e^{(E-\mu/T)}}\right\} \qquad (7)$$

where μ is the chemical potential, for our calculation we put μ=0 in Eq.(7)and g is the spin degeneracy factor. Then the energy distribution of the particles produced corresponding to temperature T is;

$$f(E,\eta)=\frac{d^2N}{P^2dPd\Omega}=\frac{g}{4\pi m^3}\frac{1}{1+e^{E/T}} \tag{8}$$

where P and E are the momentum and total energy, respectively, of a nucleon in the center of mass. Eq. (8) describes the energy distribution of the particles emitted in the rest frame of the fireball, which shows isotropic distribution. Transforming this distribution to the laboratory system, assuming that the nuclear source is moving with velocity β_{cm} with respect to the laboratory system, hence the produced particles are emitted with angle θ_L in the lab. system, then:

$$E=\gamma_{cm}(E_L-\beta_{cm}P_L\cos\theta_L) \tag{9}$$

γ_{cm} is the Lorentz factor in the center of mass system and P_L , E_L are the momentum and energy of the produced particles in the lab. system.

$$\beta_{cm}=\frac{P_L}{E_L}=\frac{\eta[t_i(t_i+2m)]^{1/2}}{m+\eta t_i} \tag{10}$$

The laboratory distribution function $f_L(E_L,\eta,\theta_L)$ describes the energy distribution of the emitted particles from a source at a given laboratory angle θ_L. The energy distribution in the laboratory system is found by integration over η and θ_L.. The energy E in the above equations is replaced by the corresponding kinetic energy t , $E=m+t$ to put the relation in an appropriate form for comparison with the experiment. Since particles emission is allowed before approaching the equilibrium state, then it is convenient to use the Vlasov equation [4] to deal with the particles energy spectra at any time of the reaction. The Vlasov Eq. has the form,

$$\frac{df}{dt}=\frac{\partial f}{\partial t}+\frac{\vec{P}}{m}\cdot\nabla_r f-\nabla_r u(r)\cdot\nabla_p f, \tag{11}$$

where $u(r)$ is a scalar potential acting among the particles. Eq.(11) may be solved by applying some approximations. First, we shall consider a pre-equilibrium state where the time derivative

(df/dt) may be approximated as($(f-f_0)/t_c$) , Where f_0 is the equilibrium distribution. Since we are dealing with a state near equilibrium, so it is convenient to consider that the rate of change of the function f is

approximately equal to that of f_0. So we replace f by f_0 in the right hand side (RHS) of Eq.(11).

Moreover, let us consider the particles as almost free so that we neglect the potential $u(r)$ in this stage of approximation. Eq.(11) then becomes.

$$f_1 = f_0 + t_c \frac{\vec{P}}{m} \cdot \vec{\nabla}_r f_0$$

$$= f_0 + t_c \frac{\vec{P}}{m} \cdot \cos\theta \frac{\partial f_0}{\partial r}. \qquad (12)$$

Here f_1 is the first order approximation of the particle spectrum, tc is the time interval required by the system to approach the equilibrium state f_0, and θ is the scattering angle, the angle between the direction of particle emission and the radial direction r. A second order approximation is obtained by using instead of f in the RHS of Eq.(11), so that

$$f_2 = f_0 + t_c \frac{P}{m} \cos\theta \frac{df_0}{dr} + (t_c \frac{P}{m} \cos\theta)^2 \frac{\partial^2 f_0}{\partial r^2}. \qquad (13)$$

By the same analogy we get the relation for the n^{th} order approximation as:

$$f_n = f_0 + \sum_{i=1}^{n} (t_c \frac{P}{m} \cos\theta)^i \frac{\partial^i f_0}{\partial r^i}, \qquad (14)$$

So that the third and fourth order approximations are:

$$f_3 = f_0 + t_c \frac{P}{m} \cos\theta \frac{\partial f_0}{\partial r} + (tc \frac{P}{m} \cos\theta)^2 \frac{\partial^2 f_0}{\partial r^2} + (tc \frac{P}{m} \cos\theta)^3 \frac{\partial^3 f_0}{\partial r^3} \qquad (15)$$

And

$$f_4 = f_0 + t_c \frac{P}{m} \cos\theta \frac{\partial f_0}{\partial r} + (tc \frac{P}{m} \cos\theta)^2 \frac{\partial^2 f_0}{\partial r^2}$$
$$+ (tc \frac{P}{m} \cos\theta)^3 \frac{\partial^3 f_0}{\partial r^3} + (tc \frac{P}{m} \cos\theta)^4 \frac{\partial^4 f_0}{\partial r^4}. \qquad (16)$$

3 Results and Discussions

The predictions of the pre-equilibrium model have been applied to calculate the angular distributions of shower (relativistic particles), grey (particles of intermitted

energy) and black (particles of low energy) particles emitted in Magnesium-Emulsion(Mg+Em) collisions at 3.6 GeV/n [Figs.((3), (4) and (5), respectively)]. The solid curves are the theoretical calculations, while the black stars are the experimental data. The momentum spectra, P , for particles produced in $d+p \rightarrow p+X$ collisions at 3.3 GeV/n and for $\cos(\theta)$ from -1 to 0.66 is shown in Fig.(6). The solid curve represents the theoretical calculations according to the pre-equilibrium model while the black stars are the experimental data.

The transverse momentum distributions for the particles produced in $p+p \rightarrow \pi + X$ at $\sqrt{s} = 23.5GeV$ and $\theta = 90^o$ and in $^{16}O+^{197}Au \rightarrow \pi + X$ at 60 GeV/n are shown in Figs.((7)and(8), respectively). The solid curves represent the pre-equilibrium model predictions, while the black stars are the experimental data. It must be noticed that the predictions of the model show global fair agreement with the experimental data. The value of the parameter t_c is found by comparison of the result of Eq. (14) with the experimental data. Experimental data are taken from HEL Cairo University and the SPIRES- SLAC data group. It is found that the reactions of higher energies need more terms in the expansion series, Eq. (14) which means that the particles at high energy reactions are produced far from the equilibrium state so we need more correction terms. Also the value of t_c increases in this case. The value of t_c is viewed via the variations, the energy and emission angle of the emitted particles. The results are summarized in Table (1). From this table one can show that fast created light particles (mostly pions) are created in the early stage of the reaction at the first collision process, *i.e:* large value of t_c. As time goes on more multiple collisions occur between the nucleons of the gas system and more momentum transfers to the system. The multiple scattering processes play the role of steering in the molecular gas system *i.e:* they draw the system towards the equilibrium state with smaller t_c. As time goes on again, more multiple collisions occur and the newly light created particles are produced in wider emission cone angles. This is followed by the emission of heavier particles, nucleons, deuterons, alpha particles. In Fig.(9) we display the proton spectra produced in *p+Cu* collisions at 1.4 GeV at emission angles 300; 450; 600 and 750, the experimental data are taken from [24]. Since the energy is not so high; it is sufficient to consider only the first terms in the series (14) with t_c =1.5, 1.05, 0.9, and 0. fm/c corresponding to the angles 300; 450; 600 and 750, respectively. The decrease of the value of t_c with increasing the angles approves that, as the system approach equilibrium, the particles are emitted in wider angles. In all previous steps, we deal with a non equilibrium system where the temperature is varying along the path of the reaction. And the system is classified into domains each is characterized by its own local equilibrium with specific temperature. As final conclusion, the thermodynamic gas model can describe the nuclear reactions in heavy ion collision using the non-equilibrium approach or the concept of domain local equilibrium.

Type of emitted particles		Shower	Gray	Black
t_c		0.00435	10^{-4}	10^{-9}
Forward	Exp.	96%	77%	56 %
	Theoretical	99.8%	65%	56%
Backward	Exp.	4%	23%	44%
	Theoretical	0.2%	35%	44%

Table 1: The calculated (forward and backward) angular distributions and t_c together with the corresponding experimental data for shower grey and black particles for Mg+Em interactions at 3.6 GeV

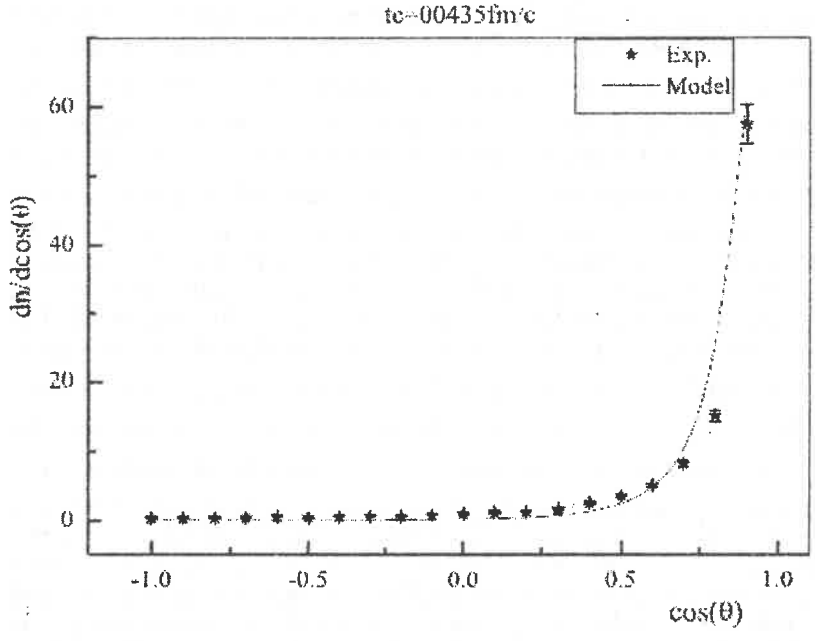

Figure 3: The angular distributions of the shower particles emitted in Mg+Em interactions at 3.6
GeV/n. The solid curve represents the model predictions, while the black stars are the experimental data which have been taken from HEL Cairo University.

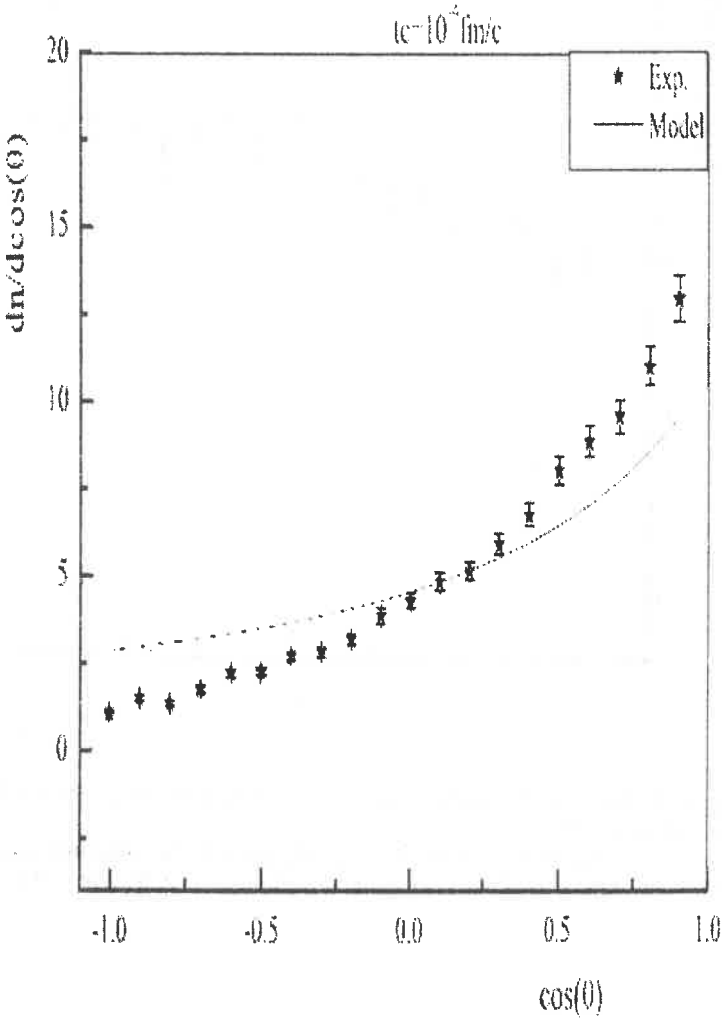

Figure 4: The angular distributions of the grey particles emitted in Mg+Em interactions at 3.6 GeV/n. The solid curve represents the model predictions, while the black stars are the experimental data which have been taken from HEL Cairo University.

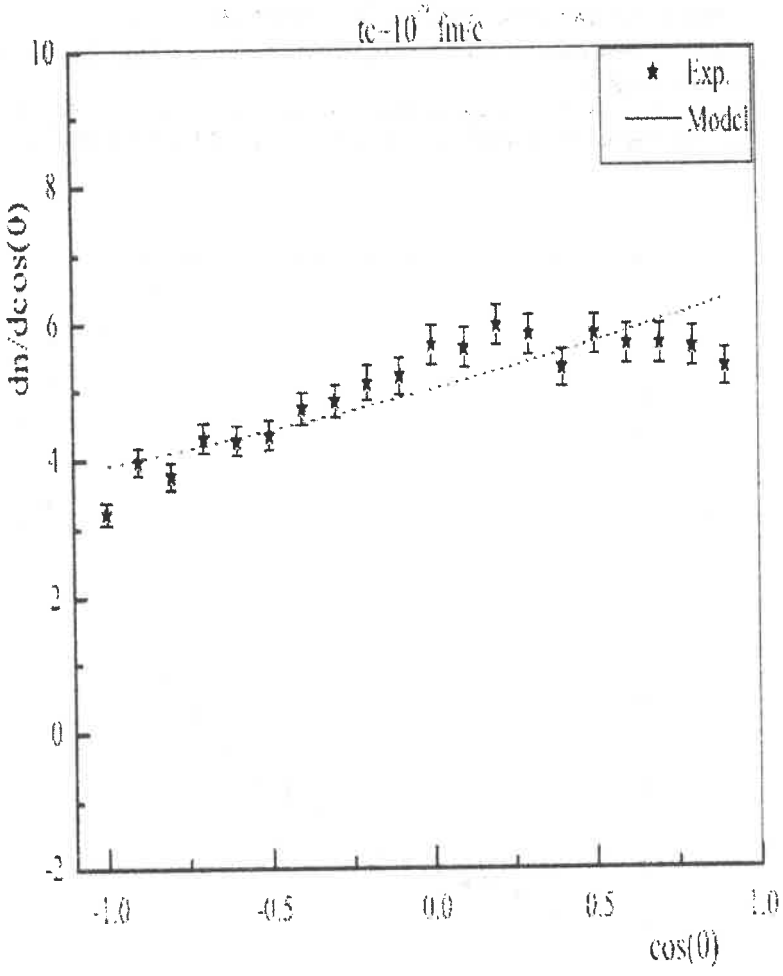

Figure 5: The angular distributions of the black particles produced in Mg+Em interactions at 3.6
GeV/n. The solid curve represents the model predictions, while the black stars are the experimental data which have been taken from HEL Cairo University.

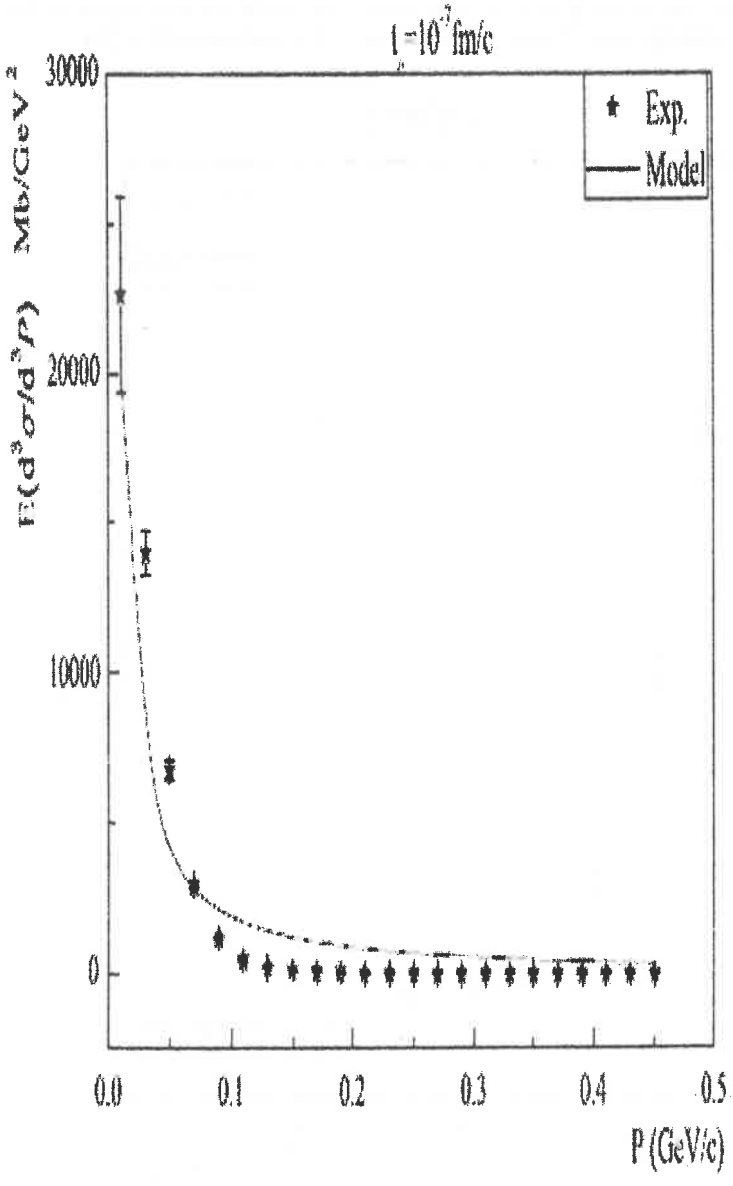

Figure 6: Momentum spectra, P , for the particles produced in $d + p \rightarrow p + X$ collisions at = 3.3

GeV/n and $\cos(\theta)$ from -1 to 0.66^0 . The solid curve represents the theoretical spectrum according to the pre-equilibrium model and the black stars represent the experimental data spectrum. The experimental data have been taken from [25].

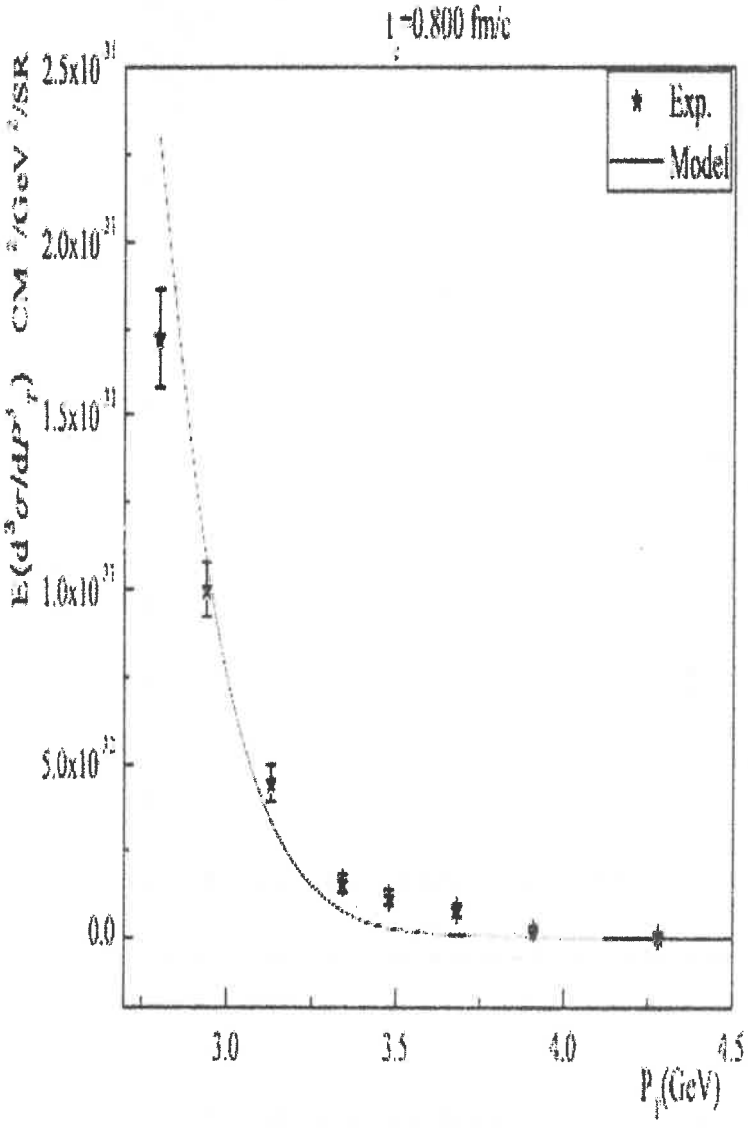

Figure 7: Transverse Momentum, PT , distribution for pion particles produced in $p+p \rightarrow \pi + X$ collisions at $\sqrt{s} = 23.5GeV$ GeV, and $\theta = 90^0$. The solid curve represents the theoretical calculations according to the pre-equilibrium model, while the stars have been the experimental data which have been taken from [26].

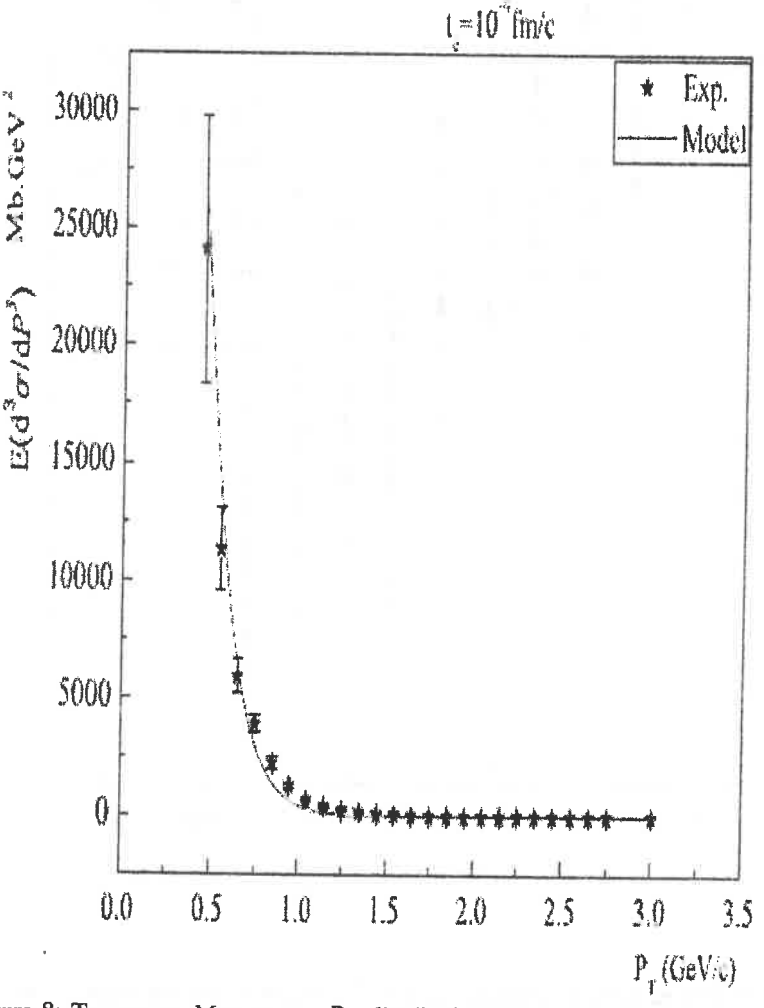

Figure 8: Transverse Momentum, P_T ,distributions for pions particles produced in $^{16}O+^{197}Au \rightarrow \pi + X$ interactions at 60 GeV/n. The solid curve represents the theoretical calculations according to the pre-equilibrium model and the black stars

represent the experimental distribution. The experimental data have been taken from [27]

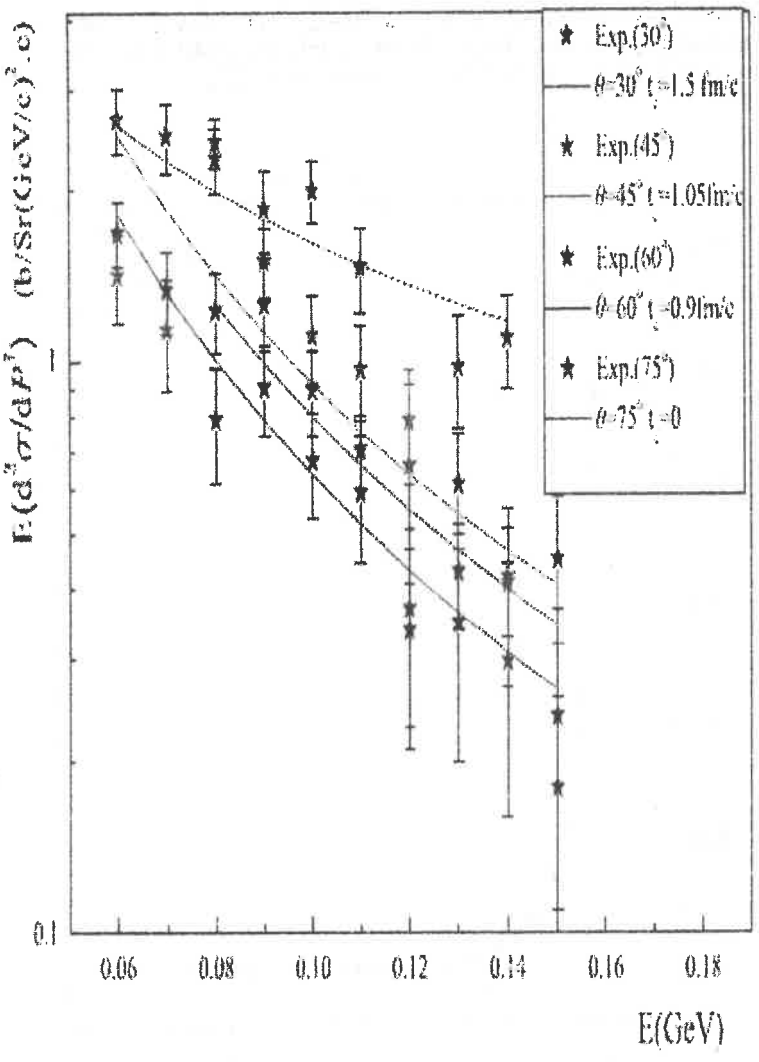

Figure 9: Proton spectra produced in $p + Cu \rightarrow p + X$ interactions at 1.4 GeV. The solid curves represent the theoretical calculations according to the

pre-equilibrium model and the star points represent the experimental data. The experimental data have been taken from [24]

4 Conclusive Remarks

1. The pre-equilibrium model with reasonable approximations may fit the experimental data of heavy ion collisions. A power series is presented to describe the nuclear density function in the frame of a thermodynamic picture. The formulation and the dynamic picture are determined by solving the Vlasov differential equation.
2. The temperature gradient in the system is determined according to the assumption that the nuclear matter has a diffuseness surface density with Gaussian distribution.
3. The temperature has minimum values around the center and near the end of the effective range of the nuclear matter. These regions are responsible for the emission of low energy particles, while fast particles are produced in the bulk region characterized by the projectile fraction parameter $\eta = 0.5$ and high temperature.
4. The power series solution is found with converging in nature. The n^{th} order term depends on the n^{th} derivative of the phase space distribution function and the *nth* power of the time parameter t_c that measures the reaction time relative to the equilibrium state as a time reference point.
5. The value of the parameter t_c is found by comparison with the experimental data.
6. It is found that reactions of higher energies need more terms in the expansion series which means that the particles at high energy reactions are produced far from the equilibrium state so we need more correction terms. Also the value of t_c increases in this case.
7. Particles emitted in the forward direction are produced in the early stage of the reaction, far from the equilibrium. Backward production comes in a later stage when the system constituents undergo multiple cascade collisions.
8. The predictions of the pre-equilibrium model have been applied to calculate the angular distributions of shower, grey and black particles emitted in Magnesium-Emulsion (Mg+Em) collisions at 3.6 GeV/n . Fair agreement with the experimental data has been obtained

References

[1] W. D. Myers. *Phys. Lett.*, A296:177{188, 1978.
[2] J. Gosset, H. H. Gutbrod, W. G. Meyer, et al. *Phys. Rev.*, C16:629, 1977.
[3] J. Gosset, J. I. Kapusta, and G. D. Westafall. *Phys. Rev.*, C18:844, 1978.
[4] G. F. Bertsch and S. Das Gupta. *Phys. Rep.*, 160:189, 1988.
[5] J. Aichelin and G. F. Bertsch. *Phys. Rev.*, C31:1730, 1985.
[6] H. Kruse, B. V. Jacak, and H. Stocker. *Phys. Rev. Lett.*, 54:289, 1985.
[7] C. Gregorie, B. Renaud, F. Sebille, et al. *Nucl. Phys.*, A465:317, 1987.
[8] T. Deal and S. Falierosyy. *Phys. Rev.*, C7:1709, 1973.
[9] J. Noble. *Ann. Phys.*, 67:98, 1971.
[10] J. Martorell et al. *Phys. Lett.*, B60:313, 1976.
[11] M. M. Islam, R. J. Luddy, and A. V. Prokudin. *Mod. Phys. Lett.*, 18:734, 2003. hep- ph/0210437.
[12] B. Abu-Ibrahim and Y. Suzuki. *Nucl.Phys.*, A728:118{132, 2003.
[13] H. F. Arellano and H. V. Von Geramb. *Phys. Rev.*, C66:024602, 2002.
[14] T. D. Cohen and D. C. Dakin. *Phys. Rev.*, C68:017001, 2003.
[15] B. Davids and S. Typel. *Phys. Rev.*, C68:045802, 2003.
[16] N. M. Hassan, N. El-Harby, and M. T. Hussein. *APH N. S. Heavy Ion Physics*, 12:33, 2000.
[17] J. U. Klaetke and K. H. Mutter. *Nucl. Phys.*, B 342:764, 1990.
[18] M. T. Hussein, A. Rabea, A. El-Naghy, and N. M. Hassan. *Progress of Theoretical Phys. Japan.*, Vol. 93 No. 3:585, 1995.
[19] G. N. Fowler, F. S. Navarra, M. Plumer, et al. *Phys. Lett.*, B214:567, 1988.
[20] M. Wellner. *Phys. Rev. Lett.*, 68:1811, 1992.
[21] B. Muller and A. Tragonov. *Phys. Rev. Lett.*, 68:3387, 1992.
[22] M. T. Hussein, N. M. Hassan, and N. Elharby. *Turk. J. Phys.*, 24:501, 2000.
[23] M. Abramowitz and I. A. Stegun. *Hanbook of Mathematical Functions*. Dover Publications, Inc.,New York, P:376, 1968.
[24] T. A. Shibata et al. *Nucl. Phys.*, A408:525{558, 1983.
[25] S. Shimansky et al. DUBNA JINR - 88-443 (88,REC.SEP.) 3p.
[26] F. W. Busser snd L. Camilleri, L. diLella, et al. *Phys. Lett.*, B 46:471{476, 1973.
[27] R. Albrecht et al. *Phys. Lett.*, B201:390, 1988.